Effects of Cyclic Behaviour during Pile Penetration on Pile Performance in Model Load Tests

S. Moriyasu[1], T. Matsumoto[2], M. Aizawa[3], S. Kobayashi[4] and S. Shimono[5]

[1]Steel Structures Research Lab, NIPPON STEEL CORPORATION, Chiba, Japan
[2,4]Graduate School of Natural Science and Technology, Kanazawa University, Ishikawa, Japan
[3,5]Toyama Prefecture, Japan (former student of Kanazawa University)

[1]E-mail: moriyasu.45e.shunsuke@jp.nipponsteel.com
[2]E-mail: matsumoto@se.kanazawa-u.ac.jp
[4]E-mail: koba@se.kanazawa-u.ac.jp

ABSTRACT: This study focuses on the effect of 'cyclic' behaviour of pile installation methods on the penetration resistance and bearing capacity of a model pile. A series of laboratory model tests were conducted to investigate this cyclic effect by comparing three kinds of piling methods: monotonic jack-in, pseudo-dynamic push-in and pull-out, i.e. 'surging', and vibratory driving in dry or saturated sand. Surging or vibratory pile driving decrease the pile penetration resistance due to negative soil dilation caused by the cyclic shearing of the soil surrounding the pile. Static load tests show that surging and vibratory pile driving provide the same or larger pile head load as the jack-in method does. Furthermore, the fluctuation of the pore water pressure strongly indicates a change in soil dilation. Both surging and vibratory pile driving prevent positive dilation more than the jack-in method due to differences in cyclic shearing and monotonic loading.

KEYWORDS: Pile installation method, Jack-in, Surging, Vibratory pile driving, Pore water pressure

1. INTRODUCTION

It has become difficult to employ the impact hammer method in urban and residential area because it causes noise and ground vibrations. Vibratory pile driving and rotary pile installation (jack-in) methods have been developed as alternatives that can install the pile with less noise and ground vibrations. Previous studies about these methods focused on soil resistance during pile penetration. In contrast, only a few studies focused on the bearing capacity of the pile installed by these methods. If the bearing capacity is clarified, these methods will become more available.

The purpose of this study is to investigate the effects of different piling methods on pile performance characteristics such as penetration resistance, bearing capacity, and load-settlement relation during the static pile load test. A significant factor is the 'cyclic' movement during pile penetration. Moriyasu et al. (2016) compared the pile behaviour between the monotonic jack-in and surging in a dry sand model. Surging refers to the cyclic push-in and pull-out movement of a pile during installation. Cyclic shearing by surging causes negative dilation around the pile shaft and soil compaction below the pile tip.

Thus, this paper focused on the effects of dynamic surging on the pile penetration resistance and bearing capacity by comparing them with the effects of pseudo-dynamic surging. A series of laboratory tests were conducted, including three kinds of piling methods (monotonic jack-in, surging and vibratory pile driving) in two sand conditions (dry or saturated).

2. EXPERIMENT DESCRIPTION

2.1 Model pile

An aluminium pipe pile with an outer diameter of 32 mm, a wall thickness of 1.3 mm, and a length of 595 mm was used as a model pile. Regarding the pile tip condition, six cases were open ended (OP), and one case was closed ended (CP). To obtain the distribution of axial forces, strain gauges were attached to the pile shaft at 6 different levels, with two strain gauges on opposite faces at each level, as shown in Figure 1(a).

The pile surface was coated with an acrylic adhesive to protect the strain gauges, and it was glued with silica sand to increase the pile shaft resistance (Figure 1(b)). The sand was the same material as the model ground.
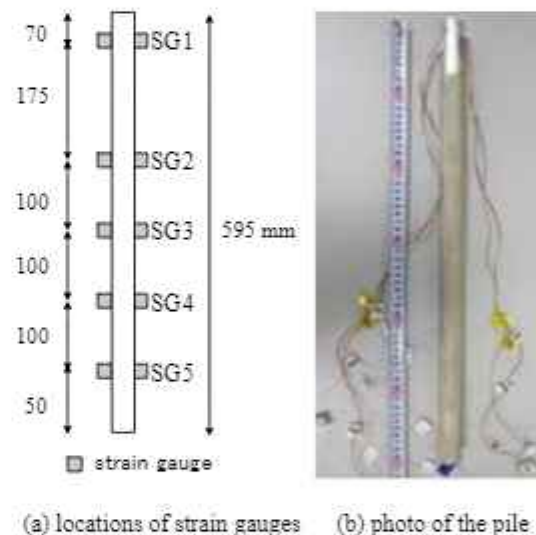

(a) locations of strain gauges   (b) photo of the pile

Figure 1 Model pile

2.2 Model ground

The material for the model ground was Silica sand #6. Table 1 lists the physical properties of the sand. Dry ground models were prepared in a rigid cylindrical soil container with a diameter of 566 mm and a height of 580 mm with 11 soil layers 50 mm thick and one layer 30 mm thick. The sand for each soil layer was put into the soil box and compacted by hand tamping to achieve a designated relative density, $D_r = 80$ %. This procedure was repeated to complete the model ground of 530 mm high.

Table 1 Physical properties of the sand

Soil particle density, ρ_s	(t/m³)	2.679
Minimum dry density, ρ_{dmin}	(t/m³)	1.366
Maximum dry density, ρ_{dmax}	(t/m³)	1.629
Maximum void ratio, e_{max}		0.962
Minimum void ratio, e_{min}		0.645
Mean particle size, D_{50}	(mm)	0.520

To prepare saturated ground models, the soil box was filled with water, and then sand was poured into the soil box and compacted as in the preparation of the dry ground models. Although $D_r = 80 \%$ was intended for the saturated ground models, only $D_r = 70 \%$ was achieved.

2.3   Experimental procedure and cases

Figures 2 and 3 show the experimental apparatuses. During pile penetration test (PPT), the pile was installed by means of a motor jack or a vibratory hammer. When the pile was penetrated to a depth of 400 mm, the PPT was finished. Subsequently, during static load test (SLT), the pile head was pushed in two or three loading cycles. At the end of the SLT, the pile extraction force was measured by extracting the pile slightly. Finally, cone penetration tests (CPTs) were carried out to investigate the soil strength profile of the model ground.
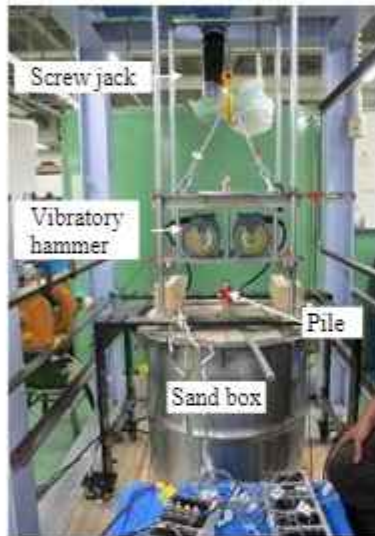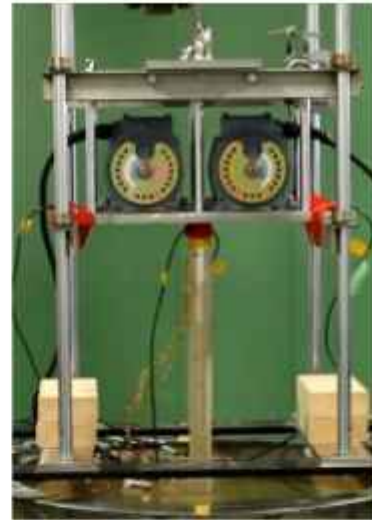

Figure 2 Loading apparatus

Figure 3 Vibratory hammer model

Table 2 shows the test cases. Case 1 to Case 4 were carried out in dry ground, while Case 5 to Case 7 were carried out in saturated ground. For each ground condition, three kinds of penetration methods were employed. The jack-in method used in Case 1 and Case 5 is a monotonic pile installation at a penetration rate of 0.2 mm/s. The surging method used in Case 2 and Case 6 is a cyclic installation using repetitions of a 2 mm jack-in and a 1 mm pull-out. In these methods, the pile was installed by using the jack without pile rotation.

In the vibration method used in Cases 3, 4, and 7, a vibratory hammer model was employed. As shown in Figure 3, the hammer has tandem rotating eccentric weights that generate vertical vibrations and cancel horizontal vibrations. The vibratory hammer has a weight of 300 N and a maximum frequency of 60 Hz. The closed-ended pile was used in Case 4, while the open-ended pile was employed in the other cases.

SLT was carried out subsequent to PPT in each case. In all cases, the pile penetration rate was 0.1 mm/s.

Table 2 Experimental cases and conditions

Case No.	1	2	3	4	5	6	7
Model ground	Dry	Dry	Dry	Dry	Saturated	Saturated	Saturated
Relative density, D_r (%)	79.9	79.9	80	80	69.5	64.3	69.5
Dry density, ρ_d (t/m³)	1.568	1.568	1.568	1.568	1.538	1.524	1.538
Pile tip condition	Open	Open	Open	Close	Open	Open	Open
Penetration method	Jack-in	Surging	Vibration	Vibration	Jack-in	Surging	Vibration
Penetration speed during PPT (mm/s)	0.2	0.2	-	-	0.2	0.2	-
Penetration speed during SLT (mm/s)	0.1	0.1	0.1	0.1	0.1	0.1	0.1
Vibration frequency (Hz)	-	-	20 to 35 Hz	20 to 35 Hz	-	-	15 to 20 Hz
Test sequence	PPT ↓ SLT ↓ CPT	PPT ↓ SLT ↓ CPT	Static loading by V.H. ↓ Vibratory penetration ↓ SLT ↓ CPT	Static loading by V.H. ↓ Vibratory penetration ↓ SLT ↓ CPT	PPT ↓ SLT ↓ CPT	PPT ↓ SLT ↓ CPT	Static loading by V.H. ↓ Vibratory penetration ↓ SLT ↓ CPT

PPT: Pile Penetration Test, SLT: Static Loading Test, CPT: Cone Penetration Test, V.H.: Vibratory Hammer

2.4 Measurements

During PPT and SLT, the pile head load, pile head displacement, and pile strains were measured. In the cases of jack-in and surging, the pile head load was measured by a load cell set between the pile head and the motor jack. On the other hand, in the case of vibration, the axial force was estimated from the strain measured near the pile head (i.e. SG level 1 in Figure 1(a)). Furthermore, a pair of acceleration transducers was attached near the pile head. In the saturated sand cases, pore water pressures were measured using the transducers located as shown in Figure 4.

2.5 Monotonic and cyclic triaxial shear tests of the sand

In order to investigate the mechanical properties of the sand, monotonic and cyclic consolidated shear tests in drained (CD) and undrained (CU) conditions were carried out.

Figure 5 shows the results of the triaxial CD tests of dense sand ($D_r = 82\%$): (a) axial strain ε_a vs. deviatoric stress q and (b) ε_a vs. volumetric strain ε_{vol} (dilatancy curve). The specimen was consolidated under a confining pressure of 100 kPa, and then, monotonic or cyclic shearing was carried out. As the result of the monotonic loading case, nonlinearity and softening behaviour are observed from the stress q – strain ε_a relationship. The internal friction angle at peak strength, ϕ_p', is 42.8° and that at the residual state, ϕ_r, is about 35°. During the cyclic loading, ε_a increases with constant q (Figure 5 (a)). In contrast, ε_{vol} does not increase, as shown in Figure 5 (b). These results mean that cyclic loading prevents soil dilation. When cyclic loading is returned to monotonic loading, the q - ε_a and the ε_a - ε_{vol} relationship returns to the curve of the monotonic loading case.

Figure 6 shows the relationship between the axial strain, ε_a, and the deviatoric stress, q, in the case of a triaxial CU test. Figure 7 shows the relationship between ε_a and the excess pore water pressure, u_e. Figure 8 shows the effective stress paths. The confining pressure of these tests was about 30 kPa. The internal frictional angle was 38 to 40°, and the shift phase angle was 28°.
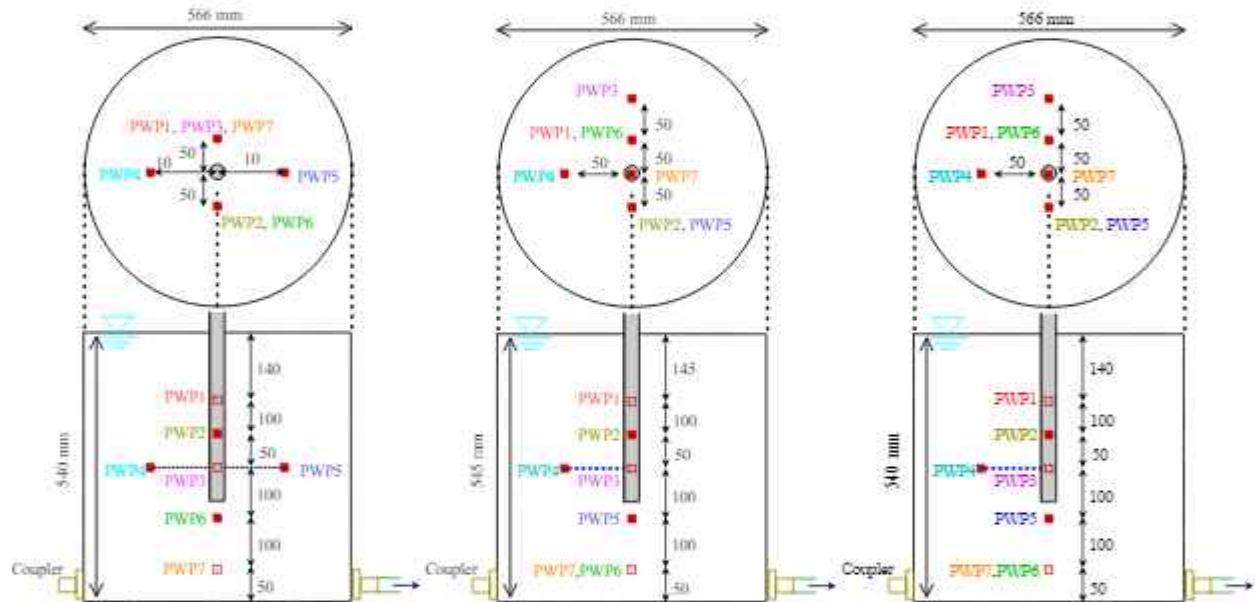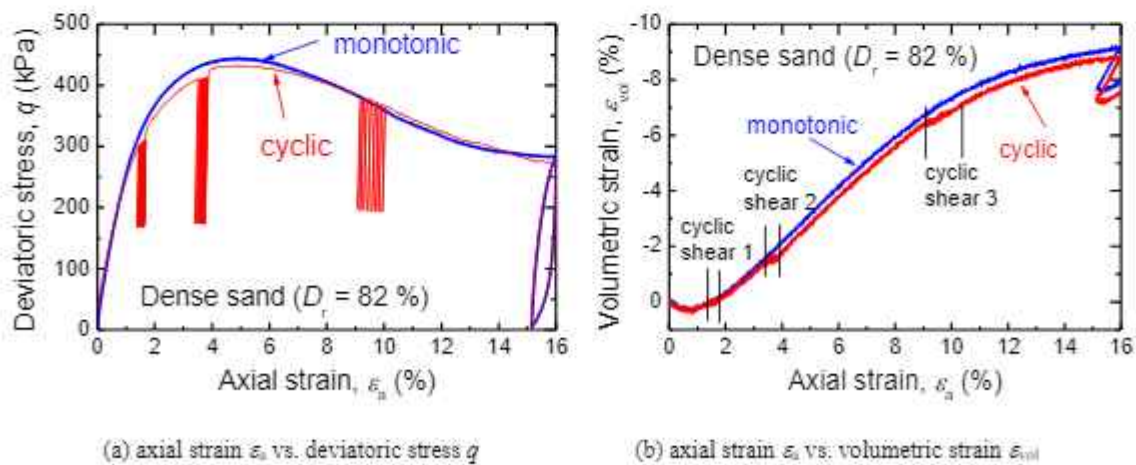

Figure 4 Locations of 7 pore water pressure (PWP) transducers in Cases 5 to 7

(a) axial strain ε_a vs. deviatoric stress q

(b) axial strain ε_a vs. volumetric strain ε_{vol}
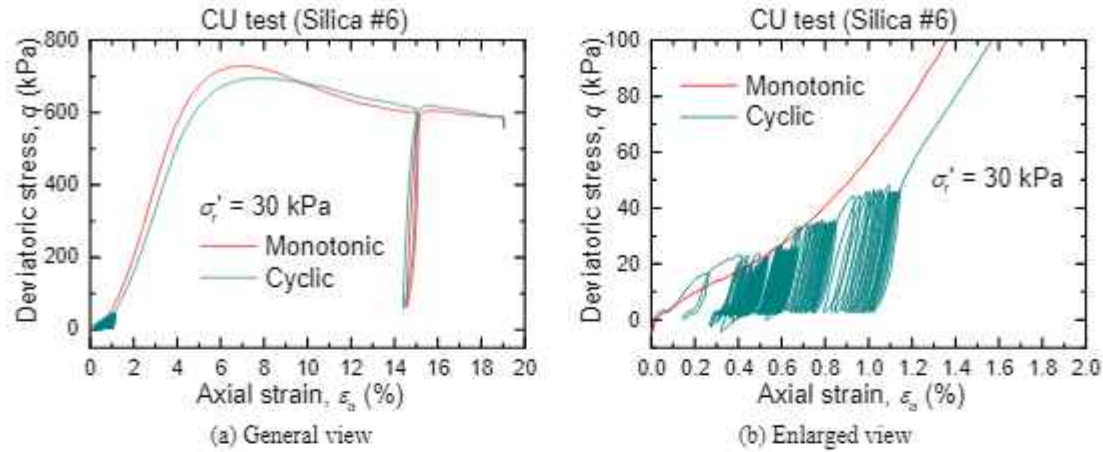
Figure 5 Results of the triaxial CD tests in dense ground

Figure 6 Relationship between the axial strain, ε_a, and the deviatoric stress, q
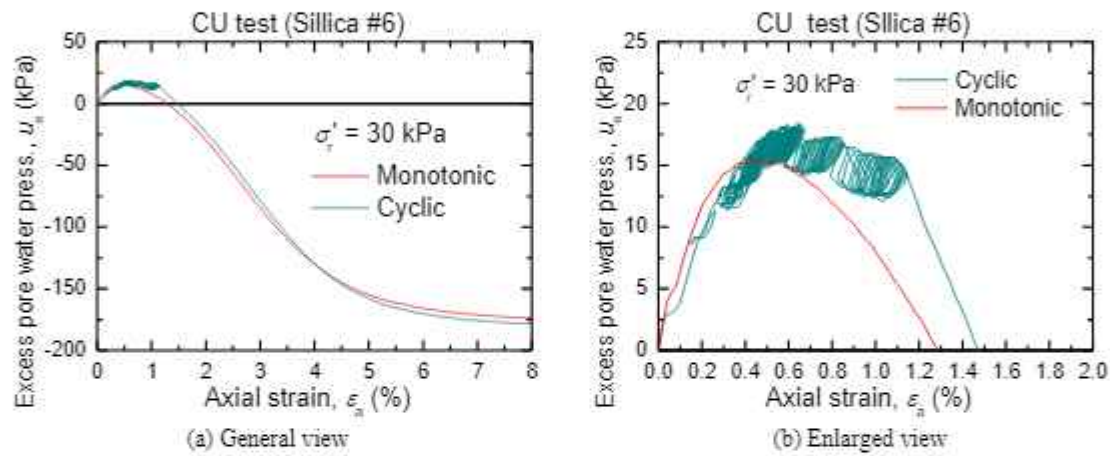

Figure 7 Relationship between the axial strain, ε_a, and the excess pore water pressure (PWP), u_e

During cyclic loading, it is seen from Figure 6 that ε_a increased as the number of loading cycles increased with each constant q. At the same time, cyclic loading generates excess pore water pressure higher than that in monotonic loading. At the monotonic loading stage after cyclic loading, the increment of u_e turned from positive to negative, because the negative dilation changed to a positive one. The change point in cyclic loading ($\varepsilon_a = 1.2$ %) was delayed behind that in the case of monotonic loading ($\varepsilon_a = 0.4$ %). Therefore, cyclic loading may act to prevent positive soil dilation. The soil behaviour is referred to discuss the experimental results later.
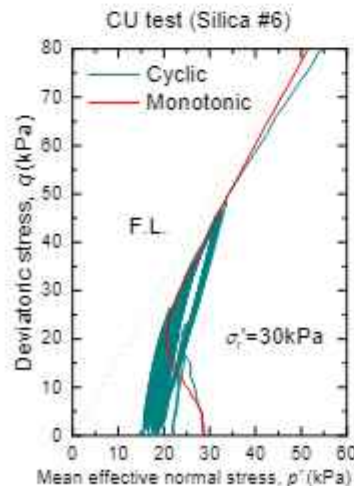
3. EXPERIMENTAL RESULTS

3.1 Results of Cone Penetration Tests in the model ground

Figure 9 shows the relationship between the vertical effective stress, σ_v', and the depth in the cases of dry and saturated grounds. It is noted that the ground water levels in Cases 5 and 7 are 100 mm below the ground surface.
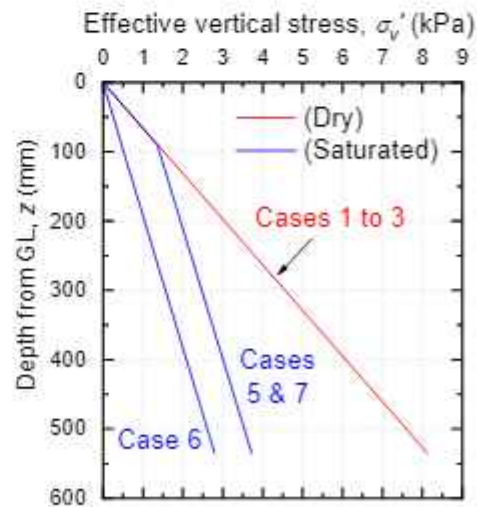

Figure 8 Effective stress channel paths

Figure 9 Vertical effective stress (GL: ground level)

Figure 10 shows the CPT tip resistance, q_c, measured in Case 2 (dry ground) and Case 6 (saturated ground). The CPTs were carried out after SLT. CPT profiles of other cases are similar to Figure 10. The q_c in saturated ground (Case 6) is smaller than that in dry ground (Case 2) due to a smaller σ_v' in the saturated ground. Furthermore, q_c may be influenced by the soil behaviour during PPT and SLT because CPT was carried out after the PPT and SLT.
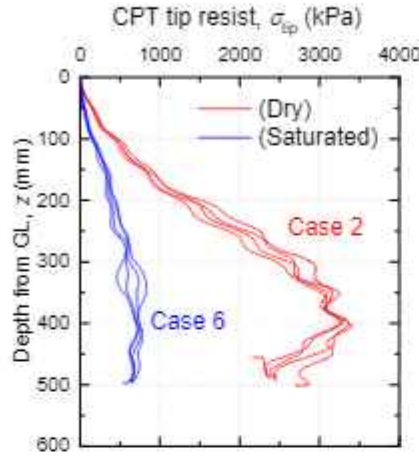

Figure 10 CPT results (GL: ground level)

3.2   Results of the pile penetration tests

Figure 11 shows the time history of the accelerations of the pile head and the ground surface 100 mm away from the pile axis during the vibratory pile penetration in Case 4. The downward acceleration is taken as positive. As shown in the figure, the acceleration of the pile head is much larger than that of the ground surface. The frequency of

the vibratory hammer was changed from 20 Hz to 35 Hz to enhance the pile penetration ability of the vibratory hammer during PPT.
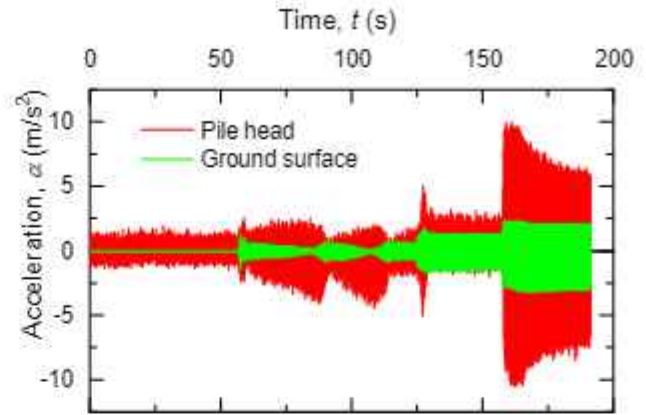

Figure 11 Acceleration during vibratory penetration

Figure 12 shows the relationship between the pile head load, P_h, and pile head displacement, w_h, in Cases 1 to 4 (dry ground). In Cases 3 and 4, P_h during PPT is similar, and at first, the pile was installed by the weight of the vibratory hammer alone. When the pile could no longer be penetrated by the weight of the hammer alone, at $w_h = 75$ mm, the operation of the vibratory hammer was started. Until the pile reached $w_h = 400$ mm, the frequency of the hammer was increased if the pile penetration decreased. P_h in Cases 3 and 4 (vibration) is smaller than that in Cases 1 and 2 once w_h exceeds 200 mm.

Figure 13 shows the relationship between P_h and w_h in Cases 5 to 7 (saturated ground). During PPT, P_h in Case 6 (surging) is slightly smaller than that in Case 5 (jack-in). In Case 7 (vibration), P_h decreases notably when f is increased to 18.3 Hz at $w_h = 400$ mm.
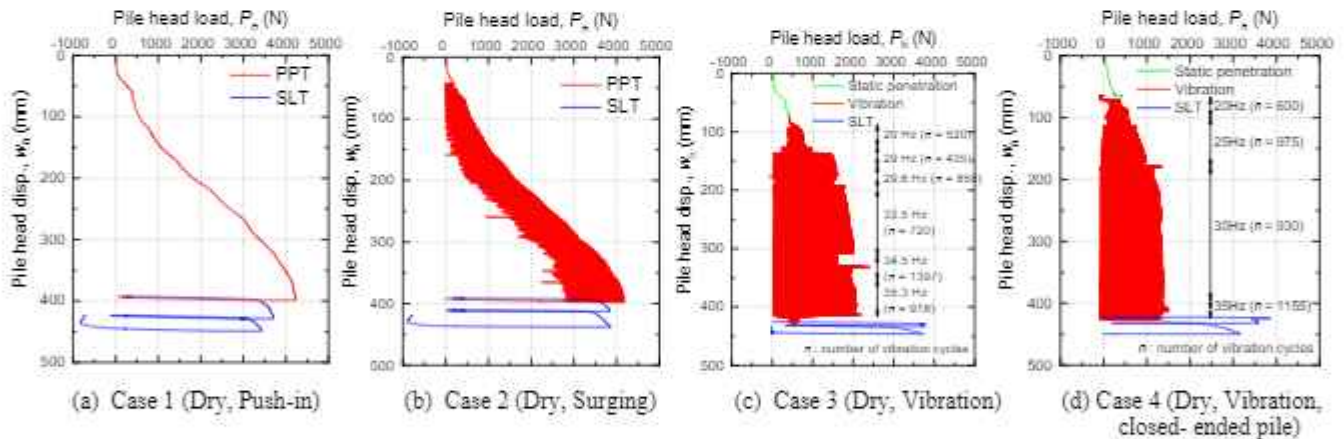

Figure 12 Relationship between the pile head load, P_h, and the pile head displacement, w_h, in Cases 1 to 4
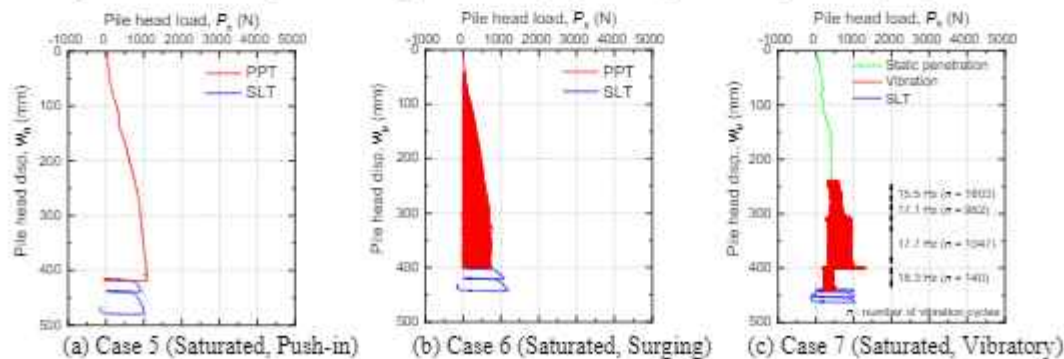

Figure 13 Relationship between the pile head load, P_h, and the pile head displacement, w_h, in Cases 5 to 7

Figure 14 shows the relationship between the pore water pressure, p, and pile head displacement, w_h, during PPT. In Case 7, p increases with w_h, and p increases dramatically when f is increased to 18.3 Hz at $w_h = 400$ mm. It is seen that soil liquefaction occurs because the excess pore water pressure corresponds to the effective vertical stress, σ_v', as shown in Figure 9. Therefore, P_b decreases with a reduction in σ_v', which is related to the soil liquefaction. As mentioned earlier, the CU test shows that cyclic shearing generates higher excess pore water pressure than monotonic loading, as shown in Figure 7. If the amplitude of the excess pore water pressure depends on the number of shearing cycles, n, it is noticed that vibration provides more shearing cycles ($n = 3800$) than surging does ($n = 350$).

Figures 15 and 16 show the comparison of the pile base resistance, P_b, and the pile shaft resistance, P_s, in dry and saturated cases, respectively. Here, the pile base resistance, P_b, is the axial force obtained from strain SG5, and the pile shaft resistance, P_s, is the difference between the pile head load, P_h, and the pile base resistance, P_b.

In dry sand, as shown in Figure 15, P_b in Case 2 (surging) is larger than that in Case 1 (jack-in), while P_s in Case 2 is smaller than that in Case 1. From the results of the cyclic triaxial CD test, it is presumed that the cyclic pile movement of surging prevents the soil dilation surrounding the pile, resulting in a reduction in the effective horizontal stresses acting on the pile shaft. As a result, P_s in Case 2 is smaller than that in Case 1. Regarding the pile base resistance, P_b, as Bolton et al. (2013) pointed out, the cavity created

below the pile tip collapses during the upward movement of the pile, and the soil below the pile tip is compacted during the following downward movement. This cyclic compaction enhances the pile base resistance notably. A similar situation is seen in Case 2. In the case of vibration (Case 3), once w_h exceeds 200 mm, P_b is dramatically smaller than it is in the other cases. A possible reason is the generation of excess pore air pressure by the vibrated pile. Watanabe et al. (2013) pointed out excess pore air pressure is generated in dry sand when it is sheared very rapidly in the triaxial compression testing. A similar situation may be occurring during PPT in Case 3 (vibration). In order to clarify the behaviour, further study is needed.

In saturated sand, as shown in Figure 16, both P_b and P_s in Case 6 (surging) are smaller than those in Case 5 (jack-in). This result corresponds to the behaviour of the water pressure, p, shown in Figure 14. In Case 5 (jack-in), the soil dilation appears clearly because p decreases with increases in w_h. The occurrence of soil dilation increases the effective soil stress and pile installation resistance. On the other hand, surging (Case 6) kept p relatively high with little variation (Figure 14 (b)). This indicates that the soil dilation is small. It is seen from the cyclic triaxial CU test that cyclic loading prevents soil dilation and generates relatively high pore water pressure. As a result, the effective horizontal stresses acting on the pile shaft are reduced. Regarding vibration (Case 7), as shown in Figure 16 (a), P_b decreases dramatically at $w_h = 400$ mm. As mentioned above, soil liquefaction occurs in this phase. Therefore, it is considered that P_b is decreased by soil liquefaction.
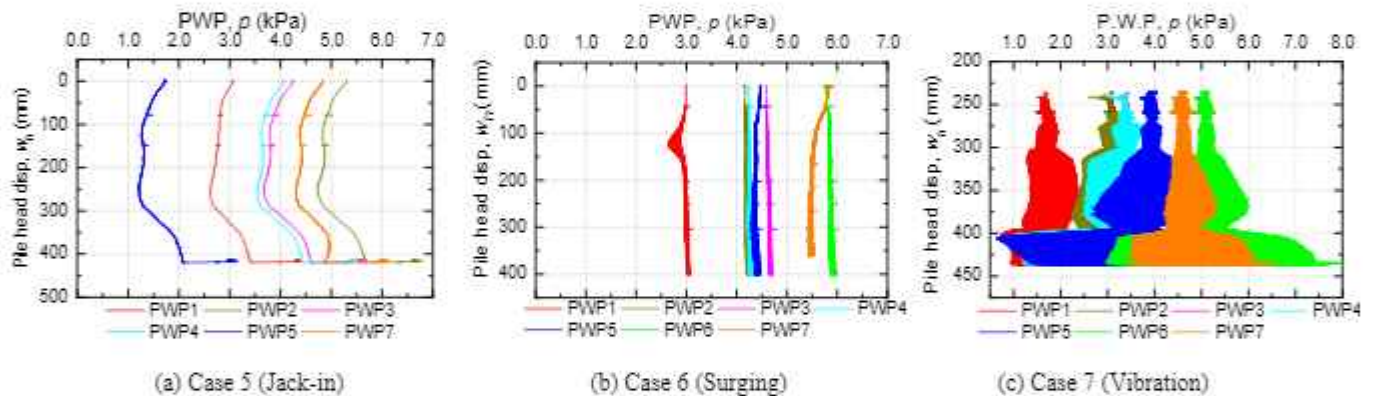

(a) Case 5 (Jack-in)   (b) Case 6 (Surging)   (c) Case 7 (Vibration)

Figure 14 Relationship between the pile head displacement, w_h, and the pore water pressure (PWP), p, during PPT

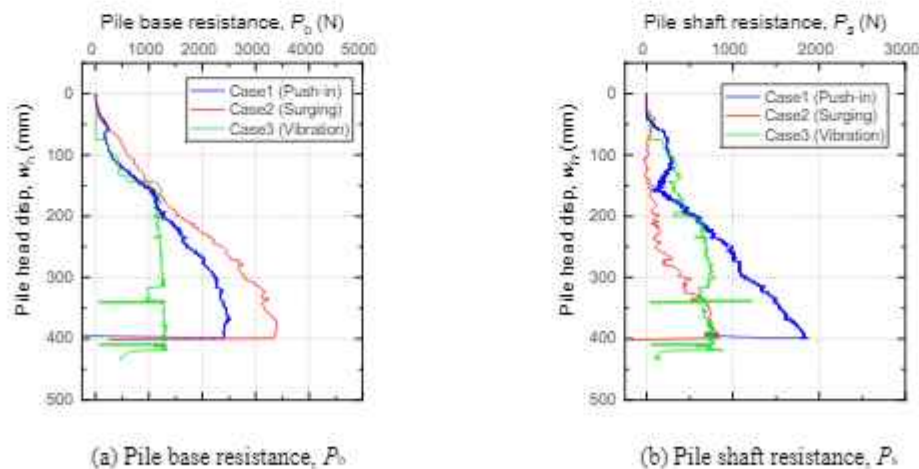(a) Pile base resistance, P_b (b) Pile shaft resistance, P_s

Figure 15 Comparison of the pile base and pile shaft resistance during PPT in Cases 1 to 3 (dry sand)

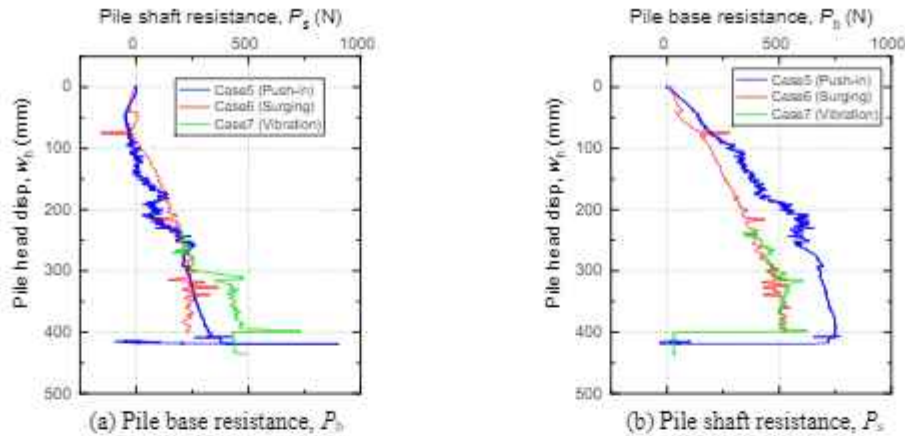(a) Pile base resistance, P_b.　　　　(b) Pile shaft resistance, P_s.

Figure 16 Comparison of the pile base and pile shaft resistance during PPT in Cases 5 to 7 (saturated sand)

3.3　Results of the static load test

The static load test was carried out subsequent to the pile penetration test. Figure 17 shows the relationship between the pile head load, P_{h_PPT}, at the end of PPT and P_{h_SLT} during the first loading cycle of SLT. P_{h_PPT} is defined as the pile head load when the pile head displacement, w_h, reaches the final PPT displacement in each case. P_{h_SLT} is the yield point of the pile head load in the initial loading cycle of SLT (P_{h_SLT} corresponds to #1 in Figure 18).
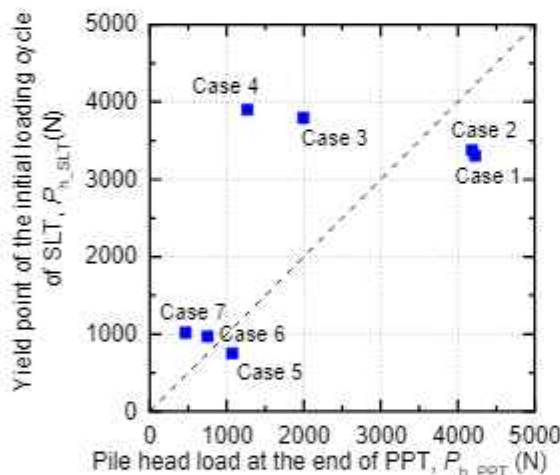

Figure 17 Relationship between the pile head load, P_{h_PPT}, at the final stage of PPT and P_{h_SLT} during the first loading cycle of SLT

In dry sand, as shown in Figure 17, P_{h_SLT} in Cases 1 (jack-in) and 2 (surging) are smaller than P_{h_PPT} in these cases. A possible reason is a difference in pile penetration rate. Watanabe et al. (2012) investigated that the failure strength and deformation modulus of sand increases with increasing loading rate. A similar behaviour may be occurring here. In contrast, P_{h_SLT} in Cases 3 (vibration) and 4 (vibration, closed-ended pile) are larger than P_{h_PPT} in these cases. As mentioned in 3.2, P_{h_PPT} may dramatically decrease by the generation of excess pore air pressure. During SLT, the excess pore air pressure disappears and the effective soil resistance is recovered.

In the saturated sand, P_{h_SLT} of Case 5 (jack-in) is smaller than P_{h_PPT}. On the other hand, P_{h_SLT} of Case 6 (surging) and Case 7 (vibration) are larger than P_{h_PPT}. As mentioned in 3.2, during PPT, the cyclic pile movement of Cases 6 and 7 prevents the soil dilation. When the SLT is started after the PPT, the loading manner is changed from cyclic to monotonic. This switch causes soil dilation, based on the result of the triaxial CU test. As a result, it is considered that P_{h_SLT} becomes larger than P_{h_PPT}.

Figure 18 (a) shows the comparison of the load-settlement curves between Case 1 (jack-in) and Case 2 (surging) in dry sand. It should be noted that the origin of the vertical axis in Figure 18 (i.e. the pile head displacement during SLT, w_{h_SLT}) is the final value of w_h during PPT due to adjusting for the different values of final w_h among the cases. #1 in each figure means the yield point in the 1st loading cycle, and #2 stands for the end point of increasing load.

As shown in Figure 18 (a), the initial pile head stiffness in Case 2 (surging) is higher than that in Case 1 (jack-in), and the yield load (#1) in Case 2 is larger than that in Case 1. Figure 19 shows the change in pile shaft resistance and pile base resistance from #1 to #2. The pile base resistance, P_b, in Case 2 (surging) is higher than that in Case 1. As mentioned above, since the surging during PPT compacts the soil beneath the pile tip, P_b during SLT becomes higher than that in jack-in.

Figure 18 (b) shows the load-settlement curves of Case 1 (jack-in), Case 3, and Case 4 (vibration). The yield loads (#1) in Cases 3 and 4 (vibration) are larger than that in Case 1. However, a softening behaviour occurs: i.e. P_h increases to 3878 N at #1 and drops immediately to P_h = 3604 N with a small increase in w_{h_SLT}. It can be seen from Figure 19 (a) that the pile shaft resistance in Case 4 decreases with increasing w_{h_SLT} (from #1 to #2), while the pile base resistance increases. This is not related to soil plugging because the behaviour occurs with both open-ended piles (Case 3) and closed-ended piles (Case 4). From the above-mentioned results, the soil conditions in the vibration case are presumed to be as shown in Figure 20. This figure explains that the soil surrounding the pile and beneath the pile tip is compacted by the large number of cyclic pile behaviours, while the soil in the outer zone is loosened. If such a soil condition is formed, then P_h at the beginning of SLT becomes high due to the compacted soil surrounding the pile. After a pile is installed by a large amount of w_{h_SLT}, the compacted soil zone reaches plastic state, and the outer soil zone contributes to pile resistance. If the soil strength of the outer zone is smaller than that of the compacted soil zone, P_h may decrease. More study is needed to clarify this hypothesis.

Figure 18 (c) shows the load-displacement curves in Cases 5 to 7 (saturated ground). The initial pile head stiffness in Case 6 (surging) is comparable to that in Case 5 (jack-in), and that in Case 7 (vibration) is higher than those in Cases 5 and 6. Converse to the results in Cases 3 and 4 (dry ground), the decrease in P_h during the 1st loading cycle does not occur in Case 7. As shown in Figure 19 (b), the pile base resistance values in Case 6 (surging) and Case 7 (vibration) are larger than that in Case 5 (jack-in). The pile shaft resistance also increases with the increase in w_{h_SLT} (from #1 to #2). Additionally, when the pile was extracted at the final stage of SLT, the extraction resistance was obtained. It can be seen from Figure 18 (c) that the extraction resistance values in Case 6 and Case 7 are comparable to that in Case 5.
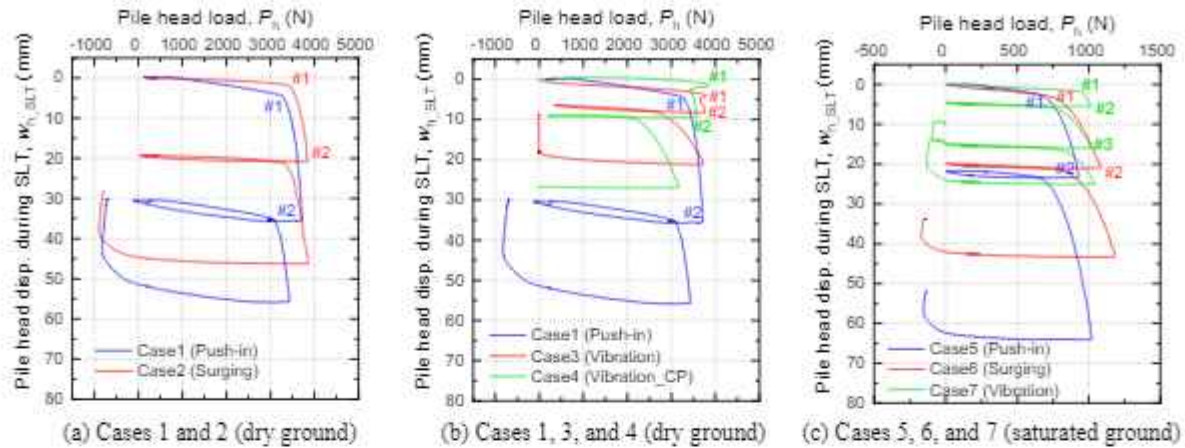
(a) Cases 1 and 2 (dry ground) (b) Cases 1, 3, and 4 (dry ground) (c) Cases 5, 6, and 7 (saturated ground)

Figure 18 Relationship between the pile head load, P_h, and the pile head displacement, w_{h_SLT}
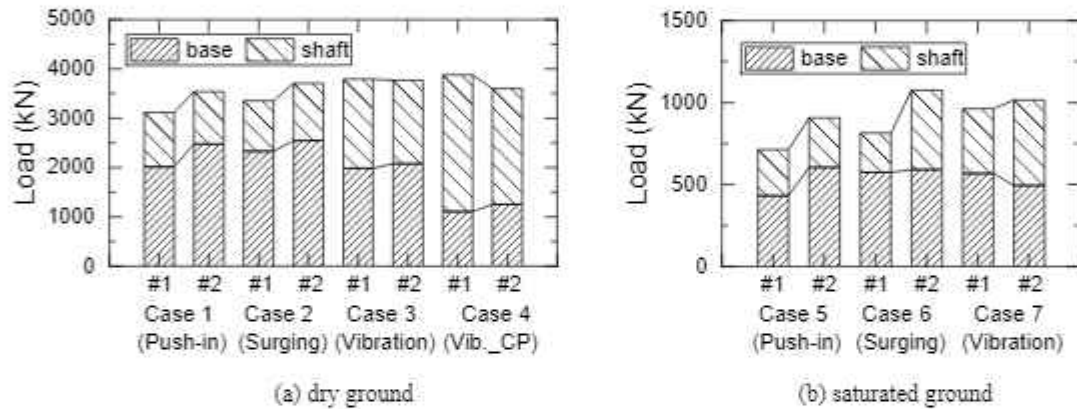

(a) dry ground (b) saturated ground

Figure 19 Change in pile shaft resistance and pile base resistance from #1 to #2 as indicated in Figure 18

Figure 21 shows the pore water pressure, p, during SLT. It can be seen from Figure 21 (a) that p in Case 5 (jack-in) is closely related to the soil dilation. Negative p (i.e. positive soil dilation) increments are generated when the pile is loaded into the compressed direction, while positive p (i.e. negative soil dilation) increments are generated when the pile was unloaded to zero.

Although the magnitudes of pore water pressures in Case 6 (surging) and Case 7 (vibration) are smaller than those in Case 5 (jack-in), they have a similar trend to those in Case 5. Furthermore, p

in Case 7 is comparable to the other cases, although the soil liquefaction occurs at the final stage of PPT. Hence, it is thought that excess pore water pressure dissipates and the ground is reconsolidated during the preparation work for SLT.

As mentioned in 2.5, it can be seen in the CU test that cyclic shearing prevents positive soil dilation. If a similar situation occurs in the laboratory pile load test, the cyclic pile movement during PPT in Case 6 (surging) and Case 7 (vibration) may prevent the positive soil dilation during SLT.
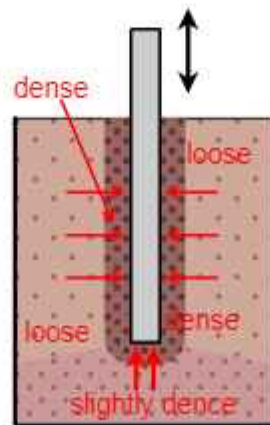

Figure 20 Schematic of changes in the soil conditions during cyclic pile penetration
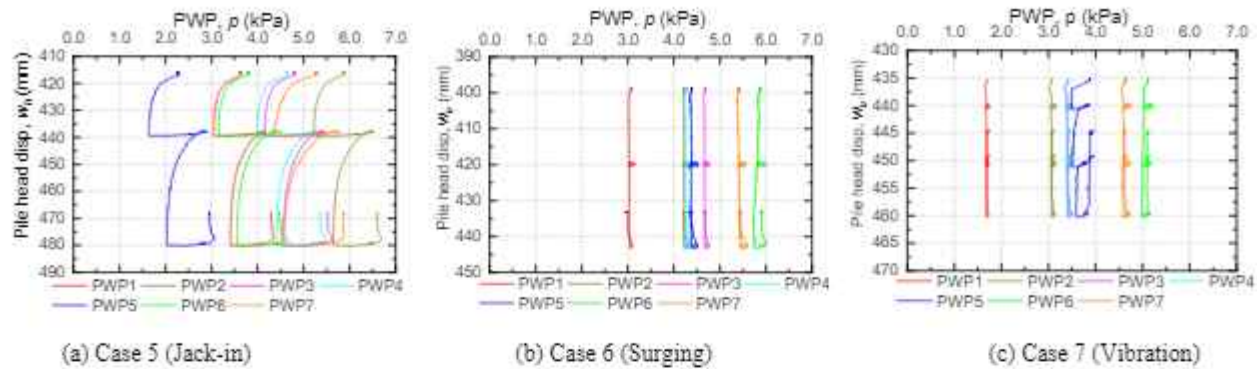
(a) Case 5 (Jack-in)   (b) Case 6 (Surging)   (c) Case 7 (Vibration)

Figure 21 Relationship between the pile head displacement, w_h, and the water pressure (PWP), p, in SLT

4. CONCLUSIONS

In order to investigate the effects of cyclic pile movement on the penetration resistance and bearing capacity, a series of laboratory model tests were conducted with different piling methods, i.e. monotonic jack-in, surging, and vibratory pile driving, in dry or saturated sand. Furthermore, triaxial CU tests of the sand used for the model ground were carried out to compare the soil behaviours under monotonic or cyclic shearing. The findings are as follows.

1) In the pile penetration tests in dry ground, the pile head load (penetration resistance) in the surging piling method is comparable to that in the jack-in piling method. The pile penetration resistance in vibratory pile driving is smaller than those in the jack-in and the surging piling methods. A possible reason for this is the generation of pore air pressure in the dry ground, although more investigation is needed.

2) In the pile penetration tests in saturated ground, the pile head load (penetration resistance) in the surging piling method was smaller than that in the jack-in piling method. The pile penetration resistance in the vibratory pile driving method was dramatically reduced due to the occurrence of soil liquefaction. Cyclic pile movements may cause negative soil dilation surrounding the pile judging from the results of cyclic shearing in the triaxial CU test. Vibratory pile driving may cause negative soil dilation that is higher than that of surging owing to the large number of loading cycles in vibratory pile driving.

3) In the static load tests in dry and saturated grounds, the pile head load of piles installed by surging or vibratory pile driving is the same or larger than that of piles installed by jack-in. In the cases of surging in saturated sand and vibratory pile driving in both dry and saturated sand, the yield load during SLT is higher than the pile head load at the end of PPT. Based on the results of the triaxial CU tests, the reason is considered to be the change of loading manner from cyclic during PPT to monotonic during SLT. After cyclic loading by surging and vibratory driving prevent soil dilation, the monotonic loading during SLT causes soil dilation and increases the soil resistance.

4) During the SLT in saturated ground, the pore water pressures are rarely changed in the cases of surging and vibratory pile driving, while negative pore water pressures are clearly observed in the case of the jack-in piling method. Since negative pore water pressure means positive soil dilation, the piles installed by jack-in cause positive soil dilation during SLT. In contrast, surging and vibratory pile driving prevent soil dilation during SLT due to the cyclic movement during PPT.

From these findings, it can be said that surging and vibratory pile driving install piles by causing negative soil dilation. Further, the bearing capacity of vibratory pile driving is comparable to that of the jack-in piling method because the cyclical pile movement enhances the pile base resistance.

5. ACKNOWLEDGEMENT

6. REFERENCES

Bolton, M.D., Haigh, S.K., Shepley, P., and D'Arezzo, F.B. (2013) "Identifying ground interaction mechanisms for press-in piles". Press-in Engineering, Proc. 4th IPA International Workshop in Singapore, pp84-95.

Moriyasu, S., Meguro, H., Matsumoto, T., Kobayashi, S., and Shimono, S. (2016) "Influence of Surging and Jack-in Pile Installation Methods on Pile Performance Observed in Model Load Tests in Dry Sand Ground", 19th Southeast Asian Geotechnical Conference & 2nd AGSSEA Conference (19SEAGC & 2AGSSEA), Kuala Lumpur.

Watanabe, K., and Sahara, M. (2012) "Effect of Loading Rate on Bearing Capacity and Soil Spring of Pile Foundations", report of Obayashi Corporation Technical Research institute, No. 76.

Watanabe, K., and Kusakabe, O. (2013) "Reappraisal of Loading Rate Effects on Sand Behaviour in View of Seismic Design for Pile Foundations" Soils and Foundations, 53(2), pp.215-231.